Supporting Information

Wu et al. 10.1073/pnas.1207356109

SI Two-Dimensional Colloidal Aggregation

Our system consists of particles with a gravitational height ($mg/k_BT \sim 2$ μm), which can therefore be considered as effectively 2D. We treat two cases, which are closed systems in which there may be triangles and open systems where there are no three particle rings containing three bonds.

Closed Structures. Closed structures with triangles are found in one-component systems where each particle can stick to every other particle and in three-component or more systems, such as our A, B, and C particles, in which each species can stick to the other two species (*ABC System*). We consider the possible clusters shown in Fig. S1*A*, in which i represents the number of particles in a cluster and α represents the number of subclusters with three particle triangles. For a group of clusters $O_{i,\alpha}$'s, the partition function $Z_{i,\alpha}$ can be written as

$$Z_{i,\alpha} = \frac{1}{N_{i,\alpha}!}\left[\frac{S}{\Lambda^2} g_{i,\alpha} e^{-\beta \Delta \varepsilon_{i,\alpha}}\right]^{N_{i,\alpha}},$$

where $N_{i,\alpha}$ is the number of clusters $O_{i,\alpha}$'s in the system, S is the surface area of the system, and Λ is a unit length that will cancel out in taking ratios. The equation $\Delta\varepsilon_{i,\alpha} = (i-1)\Delta F_p + \alpha \Delta F_p$ provides the energy of a cluster $O_{i,\alpha}$, where ΔF_p is the binding free energy of a pair of particles: $g_{i,\alpha} = \left(\frac{A_w}{\Lambda^2}\right)^{i-1}\left(\frac{\Omega_w}{\Omega_1}\right)^{\alpha}$. A_w, the "wiggling" area of a particle when bound, is determined by the maximum and minimum geometrical extent of the bound DNA links on the surface, roughly $2\pi lL$. Ω_1 is the wiggling angle of particle 3 (Fig. S1*B*) if particle 3 is bound to particle 2 and does not interact with particle 1, roughly $2\pi^*(5/6)$. Ω_w is the wiggling angle of particle 3 (Fig. S1*C*) when particle 3 is bound to both particle 1 and particle 2 simultaneously, roughly l/R. Hence, the physical meaning of $\ln(g_{i,\alpha})$ is the entropy loss of a cluster due to the inner cluster structure. As soon as we know the partition function of the clusters $O_{i,\alpha}$, the free energy of the clusters $O_{i,\alpha}$, $\Delta F_{i,\alpha}$, is straightforward and can be determined as $\Delta F_{i,\alpha} = -k_BT \ln Z_{i,\alpha}$. After that, the chemical potential of the clusters $O_{i,\alpha}$ can be written as follows:

$$\begin{aligned}\mu_{i,\alpha} &= \frac{F_{i,\alpha} + N_{i,\alpha} k_B T}{N_{i,\alpha}} \\ &= k_B T \ln\left[C_{i,\alpha}\Lambda^2\right] + (i-1+\alpha)\Delta F_p, \\ &\quad - k_B T \ln\left[\left(\frac{A_w}{\Lambda^2}\right)^{i-1}\left(\frac{\Omega_w}{\Omega_1}\right)\right]\end{aligned}$$

where $C_{i,\alpha}$ is the concentration of clusters $O_{i,\alpha}$. In thermal equilibrium,

$$\begin{cases} O_{1,0} + O_{i,0} \rightleftharpoons O_{i+1,0} \\ O_{i,\alpha} \rightleftharpoons O_{i,\alpha'} \end{cases},$$

or equivalently,

$$\begin{cases} \mu_{1,0} + \mu_{i,0} = \mu_{i+1,0} \\ \mu_{i,\alpha} = \mu_{i,\alpha'} \end{cases}.$$

After some algebra, we find

$$\begin{cases} \frac{C_{i+1,0}}{C_1 C_{i,0}} = A_w e^{-\beta\Delta F_p} \approx A_w e^{-\beta\Delta F_p} \equiv K \\ \frac{C_{i,\alpha}}{C_{i,\alpha'}} = \gamma^{\alpha-\alpha'} e^{-(\alpha-\alpha')\beta\Delta F_p} \equiv \Gamma^{\alpha-\alpha'} \end{cases},$$

where $C_1 \equiv C_{1,0}$, $\gamma \equiv \frac{\Omega_w}{\Omega_1}$, $K \equiv A_w e^{-\beta\Delta F_p}$, and $\Gamma \equiv \gamma e^{-\beta\Delta F_p}$. Then, $C_{i,\alpha}$ can be written in terms of C_1 as

$$C_{i,\alpha} = \Gamma^{\alpha} C_{i,0} = \Gamma^{\alpha} K^{i-1} C_1. \quad \textbf{[S1]}$$

Conserving the total number of particles C_p, we have that

$$C_p = \sum_{i=1}^{\infty}\sum_{\alpha=0}^{i-2} i C_{i,\alpha} = C_1 - \frac{C_1^2 K[C_1 K(\Gamma+1)-2]}{(C_1 K-1)^2 (C_1 K\Gamma - 1)^2}. \quad \textbf{[S2]}$$

Note that the upper limit of α is $(i-2)$ because a cluster with i particles can only have up to $(i-2)$ subclusters with three particles touching each other. Then, Eq. **S2** can be written in terms of the fraction of single particles or singlet fraction, $f \equiv \frac{C_1}{C_p}$, of the system as

$$\frac{1}{f} = 1 - 1\frac{C_p f K\left[C_p f K(\Gamma+1)-2\right]}{\left(C_p f K - 1\right)^2 \left(C_p f K\Gamma - 1\right)^2}. \quad \textbf{[S3]}$$

Unfortunately, Eq. **S3** does not have an analytical solution, but we can solve Eq. **S3** numerically to find the singlet fraction f.

Open Structures. For open structures, with no triangles, α is zero. Hence, Eqs. **S1** and **S2** become, respectively,

$$C_i \equiv C_{i,0} = K^{i-1} C_1^i.$$

$$C_p = \sum_{i=1}^{\infty} i C_i = \frac{C_1}{(K C_1 - 1)^2}.$$

Similarly, we have

$$f = \left(K C_p f - 1\right)^2,$$

with an analytical solution:

$$f \equiv \frac{C_1}{C_p} = \frac{1 + 2KC_p - \sqrt{1+4KC_p}}{2K^2 C_p^2}. \quad \textbf{[S4]}$$

SI Configurational Entropy Cost ΔS_p

In solution, the hybridization of DNA is governed by hydrogen bonds, the hydrophobic effect of bases, and the loss of configurational entropy in two flexible DNA single strands joining to form a rigid DNA double strand (1, 2) (Fig. S2*A*). The first two terms result in the enthalpy change ΔH^0, whereas the last term results in the entropy change ΔS^0. In addition, when the DNA strands are attached to a particle surface, the entropic cost of DNA hybridization involves a configurational entropy penalty as shown in Fig. S2*B*. dsDNA strands freely linked to a surface explore a hemisphere of area $2\pi(L + l/2)^2$. However, once the sticky ends are hybridized, the configurational freedom is reduced to a ring, which has a circumference of $2\pi\sqrt{(L+l/2)^2 - (h/2)^2}$, as well as a cross-section $\sim(l/3)^2$, where l is the length of the sticky end DNA, and a lead-lag along the circumference of $\sim(l/3)$ in

Fig. S2*B*. The extra entropy cost ΔS_p in the DNA hybridization free energy can be written as

$$\Delta S_p = k_B \ln\left[\frac{2\pi\sqrt{\left(L+\frac{l}{2}\right)^2-\left(\frac{h}{2}\right)^2}\left(\frac{l}{3}\right)^3}{\left[2\pi\left(L+\frac{l}{2}\right)^2\right]^2}\right], \qquad [S5]$$

where k_B is Boltzmann's constant. In our case, $\Delta S_p \approx -10\ k_B$.

SI Rotational Entropy ΔS_r

For a pair of spherical particles fully covered by active DNA strands, the binding can happen in any orientation as shown in Fig. S3*A*. However, for a pair of particles only partially covered by active DNA strands, the binding is limited to certain orientations between particles as shown in Fig. S3*B* (3). An active patch on each particle has to face an active patch on another particle to allow binding. The ratio of orientations that allow binding compared with all orientations is the rotational entropy cost ΔS_r.

To calculate the rotational entropy cost, we consider a simple example. Each particle only has one DNA strand and is held together with a surface separation h as shown in Fig. S3*C*. Before bonding, each particle can have any orientation, a solid angle of 4π, or, equivalently, a point can be anywhere on the $A_{\text{surface}} = 4\pi(R + h/2)^2$ area of the surface. Now, consider two particles whose centers are arranged in a certain direction. In order for the particles to bind, the single DNA on one particle must be located near the other particle close to the line connecting the particles' centers. The same is true for the DNA on the second particle. The maximum distance that the DNA strand can extend in any direction is $\sim(L + l/2)$. Thus, a patch of area $\sim\pi(L + l/2)^2$ on one particle must touch or overlap a similar patch on the second particle to allow binding. The "active" area for a single DNA on a particle surface is $A_{\text{DNA}} \sim \pi(L + l/2)^2$. The ratio of allowed orientations bound vs. unbound is $A_{\text{DNA}}/A_{\text{surface}}$ per particle. The entropy loss for binding the two particles together is $\Delta S_r = 2k_B \ln\left(\frac{A_{\text{DNA}}}{A_{\text{surface}}}\right)$.

For particles with many DNA strands, the rotational entropy can be determined in a similar way. We calculate the fraction of area covered by the active patches associated with DNA strands, ϕ. The fraction of the area not covered by one DNA strand is $1 - A_{\text{DNA}}/A_{\text{surface}}$. The average fraction of area not covered by N_{tot} DNA strands, where N_{tot} is the total number of active DNA strands on particle surface, placed randomly on the surface is $(1-A_{\text{DNA}}/A_{\text{surface}})^{N_{tot}}$. Therefore, the fraction of area covered by N_{tot} DNA strands is

$$\varphi \approx 1 - \left(1 - \frac{A_{\text{DNA}}}{A_{\text{surface}}}\right)^{N_{tot}}.$$

In our case, $A_{\text{DNA}} = \pi[(L + l/2)^2 - (h/2)^2]$, $A_{\text{surface}} = 4\pi(R_p + h/2)^2$, where $L \approx 15$ nm is the length of the backbone dsDNA, $l \approx 3.6$ nm is the length of the sticky end DNA, and R_p is the particle radius. $N_{tot} = N_t\chi$, where $N_t = 69{,}800 \pm 4{,}800$, is the total DNA coverage and χ is the ratio of active DNA strands on a particle surface. The entropy loss on binding is just the log of the fractional coverage per particle. The rotational entropy loss is

$$\Delta S_r = 2k_B \ln\left[1 - \left(1 - \frac{A_{\text{DNA}}}{A_{\text{surface}}}\right)^{N_{tot}}\right]. \qquad [S6]$$

In our case,

$$\Delta S_r = 2k_B \ln\left\{1 - \left[1 - \frac{\pi\left[\left(L+\frac{l}{2}\right)^2 - \left(\frac{h}{2}\right)^2\right]}{4\pi(Rp + h/2)^2}\right]^{N_t\chi}\right\}. \qquad [S7]$$

SI Binding Free Energy of a Pair of cDNA-Coated Particles, ΔF_p

We consider the DNA binding between particles surfaces as shown in Fig. S4. Because the DNA sticky ends are attached to the particle surface via dsDNA backbones, the binding free energy of hybridization ΔF^0 can be determined as $\Delta F^0 = \Delta H^0 - T(\Delta S^0 + \Delta S_p)$, where ΔH^0 is the enthalpy due to the hydrogen bonds of DNA bases and their hydrophobic interactions. ΔS^0 is the entropy loss in going from flexible ssDNA to rigid dsDNA, and ΔS_p is the configurational entropy loss shown in Fig. S2*B*.

We treat the partition function in a mean field approximation. First, we consider the partition function of just one DNA strand $Z_{S,1}$:

$$Z_{S,1} = 1 + g_b e^{-\beta\Delta F^\circ}.$$

The first term indicates the unbound state, whereas the second term indicates the bound states. The term g_b accounts for the fact that a DNA strand on one particle surface has a multiplicity of partners, g_b of them, on the complementary particle surface, each of which has the binding free energy ΔF^0. From the single-strand partition function, within the mean field approximation (uncorrelated bonds), the total partition function for a pair of complementary particles is

$$Z_s \approx \left(1 + g_b e^{-\beta\Delta F^\circ}\right)^{N_b}, \qquad [S8]$$

where N_b is the number of DNA strands that have the potential to form interparticle DNA bonds (1, 2). From the partition function, we calculate the binding free energy for a pair of complementary particles (1, 2):

$$\Delta F_{p,DNA} = -k_B T \ln[Z_s - 1]$$

$$\approx -k_B T \ln\left[\left(1 + g_b e^{-\beta\Delta F^\circ}\right)^{N_b} - 1\right].$$

The rotational entropy cost, Eq. **S6**, contributes $-T\Delta S_r$ to the binding free energy of a pair of complementary particles (3). Hence, the total binding free energy of a pair of cDNA-coated particles can be written as

$$\Delta F_p \approx -k_B T \ln\left[\left(1 + g_b e^{-\beta\Delta F^\circ}\right)^{N_b} - 1\right] - T\Delta S_r. \qquad [S9]$$

SI Computations of g_b and N_b

To determine the values of g_b and N_b for each χ, we perform a simple computation. Fig. S5*A* is the schematic diagram of our computation. We randomly place χN_t points on the surface of each of sphere, P1 and P2 (4). N_t is the total number of DNA strands on our particles, in our case, $N_t = 69{,}800$. The radius of each sphere is $R_p = 980$ nm. We hold these two spheres together with the surface separation $h = 16.8$ nm. Then, we determine g_b and N_b of this configuration by counting all of the possible binding pairs between P1 and P2. We average over 1,000 configurations to determine $\langle g_b\rangle$ and $\langle N_b\rangle$. The algorithm of our computation is as follows:

i) Randomly place χN_t points on the surface of each of P1 and P2 (4).
ii) Place P1 and P2 with a surface separation h.
iii) Pick a point i on P1, and calculate the distances, r_{ij}'s, between the point i on P1 and all the points j on P2.

iv) If r_{ij}'s $\leq (2L + l)$, add 1 to $g_{b,i}$, the binding degeneracy for the point i on P1.
v) Repeat step *iii* and step *iv* for all the points i on P1.
vi) Assign the average of nonzero $g_{b,i}$'s to g_b, the binding degeneracy for this configuration.
vii) Assign the number of nonzero $g_{b,i}$'s to N_b, the number of DNA bonds for this configuration.

The computation results are shown in Fig. S5*B*. For high DNA coverage, $\chi \geq 0.2$, there are many overlapping DNA strands between a pair of particles. Hence, g_b and N_b are proportional to χ. This was the approximation used in our previous calculations (1, 2). However, when $\chi < 0.2$, g_b and N_b are proportional to χ^2 rather than to χ. For the present paper, we numerically compute g_b and N_b as described above.

SI ABC System

For a three-component system as in Fig. S6*A*, the binding configurations are more fruitful than for a two-component system and result in higher melting temperatures as shown in Fig. S6*B*. The extra binding configurations can be attributed to two effects: (*i*) the 2/3 effect and (*ii*) the triangle effect.

Two-Thirds Effect. In the two-component system (A + B, B + C, or A + C system), each particle can interact with 1/2 of the other particles in the system (e.g., A cannot bind to A). However, in the three-component system (A + B + C system), each particle can interact with 2/3 of the other particles (e.g., A can bind either to B or to C). If all concentrations and reaction rates are the same, the effect is to replace the equilibrium constant K by $(3/2)^2K$. We have the same concentration of each of A, B, and C in our A + B + C system as in our binary systems; thus, the total concentration is increased by 3/2. Including these effects accounts for a change of 0.2 °C in our melting curves comparing the two-component system with the three-component system.

To actually calculate the 2/3 effect of the ABC system, we use Eq. **S4** of our model for the Watson–Crick system to plot the melting curves of A + B, B + C, and A + C systems. As shown in Fig. S6*A*, the A + B, B + C, and A + C systems have the DNA coverages $\chi_{AB} = 0.18, \chi_{BC} = 0.20$, and $\chi_{AC} = 0.23$, respectively. The enthalpy and entropy of the hybridization of sticky ends S_1 and S_1' are $\Delta H^\circ_{S_1,S_1'} = -328,000\text{J/mol}$ and $\Delta S^\circ_{S_1,S_1'} = -967\text{J/molK}$, respectively (5). The enthalpy and entropy of the hybridization of sticky ends S_2 and S_2' are $\Delta H^\circ_{S_2,S_2'} = -326,000\text{J/mol}$ and $\Delta S^\circ_{S_2,S_2'} = -957\text{J/molK}$, respectively (5). The enthalpy and entropy of the hybridization of sticky ends S_3 and S_3' are $\Delta H^\circ_{S_3,S_3'} = -332,000\text{J/mol}$ and $\Delta S^\circ_{S_3,S_3'} = -975\text{J/molK}$, respectively (5). The particle concentration of each species in either the A + B, B + C, A + C, or A + B + C system are all $C_p/2 = 0.005\ \mu\text{m}^{-2}$; thus, the total particle concentration for the A + B, B + C, or A +C system is $C_p = 0.01\ \mu\text{m}^{-2}$ and the total particle concentration for the A + B + C system is $\frac{3}{2}C_p = 0.015\mu\text{m}^{-2}$. After determining the relevant parameters, we are able to use Eq. **S4** to plot the melting curves for each of the A + B, B + C, and A + C systems as shown in Fig. S6*B*, and therefore to determine each melting temperature.

To change the above calculation from a two-component system (A + B, B + C, or A + C system) to a three-component system (A + B + C system), we simply replace the equilibrium constant K by $(3/2)^2 K$ and the total particle concentration C_p by $(3/2)C_p$ in Eq. **S4**. Then, we can easily find the melting temperature of the ABC system and that the shift of the melting temperature due to the 2/3 effect is ~0.2 °C.

Triangle Effect. From the discussion of systems with triangle structures (Eq. **S3**), we can determine the melting curve of the A + B + C system due to the triangle effect as

$$f_{ABC} = \frac{1}{3}(f_{AB} + f_{BC} + f_{AC}), \qquad \textbf{[S10]}$$

where f_{AB}, f_{BC}, and f_{AC} are determined from Eq. **S3** using the same sets of parameters used in plotting the melting curves of the A + B, B + C, and A + C systems, except the total particle concentration is increased from C_p to $3(C_p/2)$ because the A + B + C system has particles A, B, and C, each of which has particle concentration $C_p/2 = 0.005\ \mu\text{m}^{-2}$. The extra structure-related parameter γ is taken to be $\gamma = \frac{\Omega_w}{2\pi}$, where the wiggling angle of particle 3 in Fig. S1*C* is estimated to be $\Omega_w \approx \arccos\left[\frac{(2R_p)^2+(2R_p+2L+l)^2-R_p^2}{2(2R_p)(2R_p+2L+l)}\right]$ and $R_p \approx 980$ nm is the particle radius, $L \approx 15$ nm is the length of our dsDNA backbone, and $l \approx 3.6$ nm is the length of our hybridized DNA sticky end. Compared with the melting curve of the two-component system (A + B, B + C, or A + C system), we find that the shift of the melting temperature of the A + B + C system due to the triangle effect is ~0.6 °C.

Summary. To determine the melting curve of the A + B +C system, including both the "2/3" effect and the "triangle" effect, we take Eq. **S10** and replace the equilibrium constant K by $(3/2)^2K$. The melting curve for the A + B + C system is plotted in Fig. S6*B*. From Fig. S6*B*, we see that the melting temperature shift due to the extra binding configurations is ~0.8 °C, which is ~0.2 °C from the 2/3 effect and ~0.6 °C from the triangle effect.

SI Thermodynamic Model of Dual-Phase Materials

To demonstrate further that our model provides a guide for designing systems with polygamous particles, we use our model to predict the melting curve of our dual-phase system, the design of which is shown in Fig. S7*A*. In the dual-phase system, we have two complementary pairs of DNA. We use the same set of parameters as previously, except that the particle radius R_p is changed to $R_p \approx 500$ nm and the total DNA coverage N_t is changed to $N_t = 22{,}000 \pm 2{,}200$ (1, 2), because the particle used in the dual-phase material experiment is a 1-μm magnetic particle instead of a 2-μm polystyrene particle. The rotational entropy is modified from Eq. **S6** to

$$\Delta S_r(\chi_1,\chi_2) = k_B \ln\left[1-\left(1-\frac{A_{DNA}}{A_{surface}}\right)\right]^{N_t\chi_1} + k_B \ln\left[1-\left(1-\frac{A_{DNA}}{A_{surface}}\right)\right]^{N_t\chi_2}$$

for a pair of complementary particles with active DNA coverages of χ_1 and χ_2, respectively. We also recompute g_b's and N_b's for the new particles, $g_{b,XY} \approx 7, N_{b,XY} \approx 163, g_{b,YZ} \approx 6$, and $N_{b,YZ} \approx 22$. The enthalpy and entropy of the hybridization of sticky ends S_1 and S_1' are $\Delta H^\circ_{S_1,S_1'} = -328,000\text{J/mol}$ and $\Delta S^\circ_{S_1,S_1'} = -967\text{J/molK}$, respectively (5). The enthalpy and entropy of the hybridization of sticky ends S_3 and S_3' are $\Delta H^\circ_{S_3,S_3'} = -332,000\text{J/mol}$ and $\Delta S^\circ_{S_3,S_3'} = -975\text{J/molK}$, respectively (5). Particle concentrations of X, Y, and Z are $n_X = 0.006\ \mu\text{m}^{-2}$, $n_Y = 0.03\ \mu\text{m}^{-2}$, and $n_Z = 0.06\ \mu\text{m}^{-2}$, respectively. After collecting all the parameters, the melting curves of X-Y, f_{XY}, and Y-Z, f_{YZ}, can be determined from Eq. **S4**. Then, the total melting curve f_{XYZ} can be written as

$$f_{XYZ} = \frac{n_X + n_Y}{n_X + n_Y + n_Z} f_{XY} + \frac{n_Z}{n_X + n_Y + n_Z} f_{YZ}.$$

The melting curve f_{XYZ} is shown Fig. S7*B*, along with the experimental results. The good agreement shows that our simple mean field model is sufficient to predict in a semiquantitative manner the temperature-dependent hybridization of somewhat complex systems.

1. Dreyfus R, et al. (2009) Simple quantitative model for the reversible association of DNA coated colloids. *Phys Rev Lett* 102(4):048301.
2. Dreyfus R, et al. (2010) Aggregation-disaggregation transition of DNA-coated colloids: Experiments and theory. *Phys Rev E Stat Nonlin Soft Matter Phys* 81(4 Pt 1):041404.
3. Biancaniello PL, Kim AJ, Crocker JC (2005) Colloidal interactions and self-assembly using DNA hybridization. *Phys Rev Lett* 94(5):058302.
4. Press WH, Teukolsky SA, Vetterling WT, Flannery BP (2007) *Numerical Recipes: The Art of Scientific Computing* (Cambridge Univ Press, New York), Chap 21, pp 1097–1159.
5. SantaLucia J, Jr. (1998) A unified view of polymer, dumbbell, and oligonucleotide DNA nearest-neighbor thermodynamics. *Proc Natl Acad Sci USA* 95(4):1460–1465.

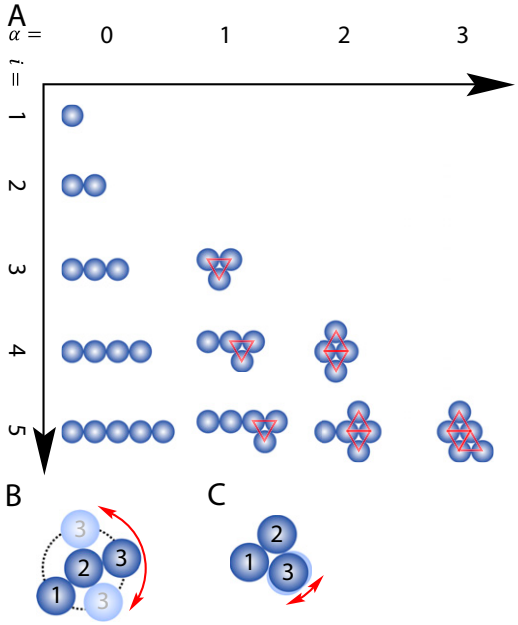

Fig. S1. (*A*) Cluster identification in terms of size or number of particles, *i* and α, and the number of subclusters with triangles (three particles bound to each other). (*B*) Wiggling angle, used to calculate entropy, of a particle bound to only one particle. (*C*) Wiggling angle of a particle bound to two particles simultaneously.

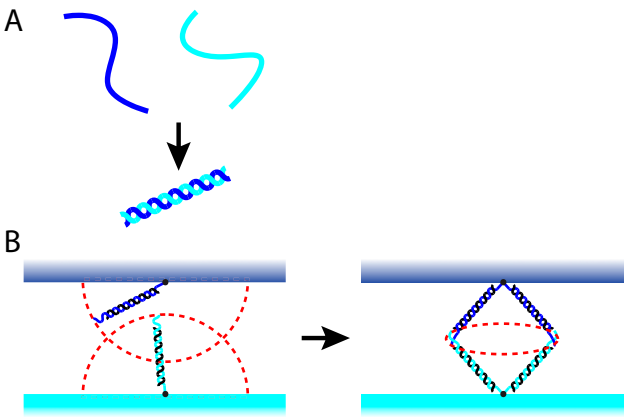

Fig. S2. DNA entropy losses from hybridization. (*A*) Entropy loss in going from two flexible single strands to one rigid double strand. (*B*) dsDNA with one end freely jointed on a surface entropy can have a hemisphere of configurations. When bound to dsDNA from another surface, the configurations are restricted to a ring.

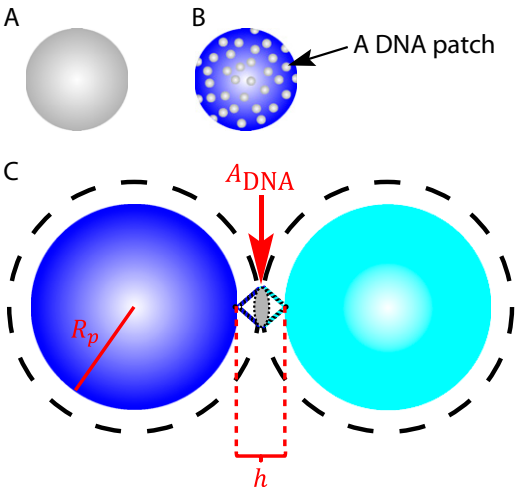

Fig. S3. Rotational entropy of spherical particles. (*A*) Particle fully covered by DNA. (*B*) Particle partially covered by DNA. Gray areas are "active" patches of area $\sim \pi(L + l/2)^2$. (*C*) Particles each with a single DNA strand. The allowed configurations for binding require the overlap of two active patches, greatly reducing the configurations allowed without binding.

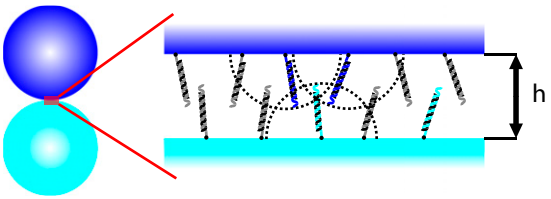

Fig. S4. Blow-up of binding region between two DNA-coated colloidal particles. We can change coverage with active and neutral DNA strands. Here, blue and cyan sticky ends are complementary to each other and are active, whereas the gray strands are neutral DNA and inactive.

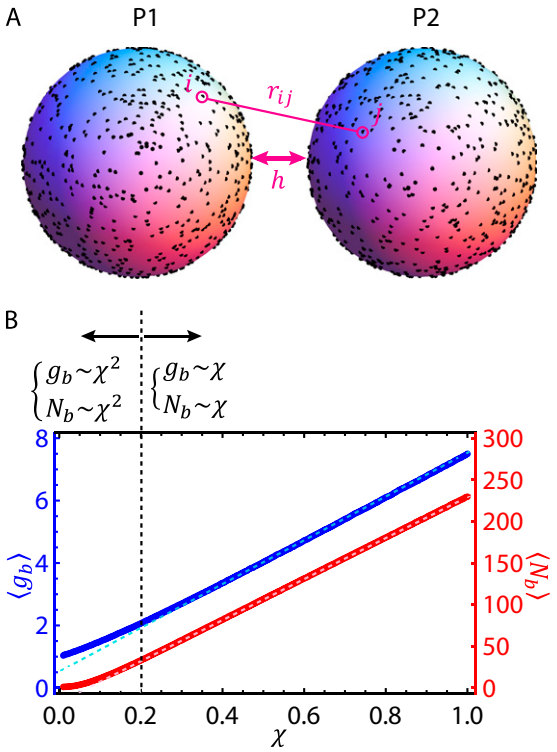

Fig. S5. (*A*) Computation of g_b, the number of DNA strands on one colloid accessible for binding to a single DNA on a complementary colloid, and N_b, the total number of possible bonds between complementary colloids. Black dots are randomly distributed DNA strands, and surface-surface separation, h, is comparable to strand length when particles bind. (*B*) $\langle g_b \rangle$ (blue) and $\langle g_b \rangle$ (red) as a function of χ, the fraction of total possible DNA coverage. At high DNA coverage, both $\langle g_b \rangle$ and $\langle N_b \rangle$ are proportional to χ, whereas at low DNA coverage, both $\langle g_b \rangle$ and $\langle N_b \rangle$ are proportional to χ^2. The dashed lines indicate $g_b \sim \chi$ and $N_b \sim \chi$.

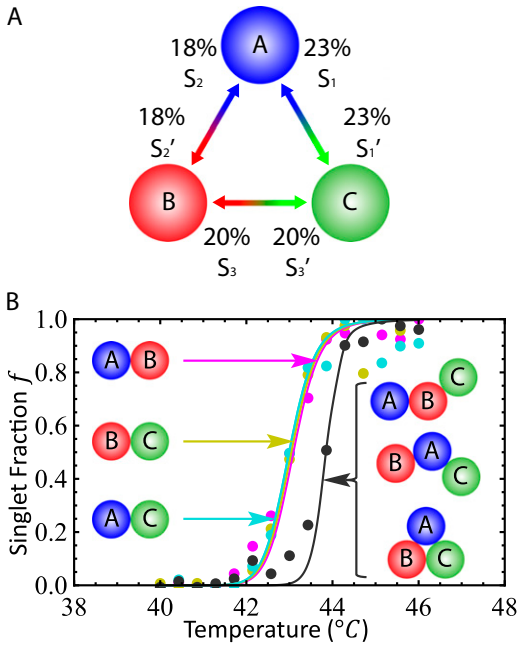

Fig. S6. A + B + C system. (*A*) Interaction diagram of A, B, and C. (*B*) Melting curves of A + B (pink), B + C (yellow-green), A + C (cyan), and A + B + C (black) systems. The dots are the experimental data. The solid curves are the model plots.

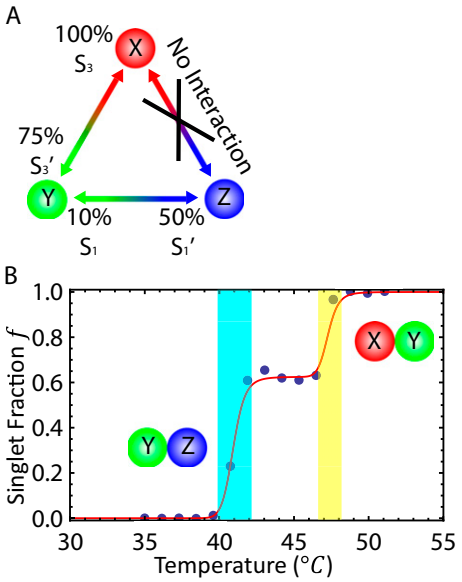

Fig. S7. Dual-phase materials. (*A*) Interaction diagram of X, Y, and Z. (*B*) Equilibrium melting curves for our dual-phase materials. The dots are the data. The solid curve is the model. Slow cooling from 50 °C to 35 °C gives isolated clusters of X surrounded by Y surrounded by Z. A rapid quench gives an extended elastic gel.